Jurnal Teknologi Kedirgantaraan (JTK)
Vol. 10, No. 1, February 2025, page. 89 – 98
ISSN: 2528-2778 (Print); 2684-9704 (Online)
https://doi.org/10.35894/jtk.v10i1.259

JTK
Jurnal Teknologi Kedirgantaraan
(Journal of Aeronautical Engineering)

Transient FSI Simulation for Aeroelastic Evaluation of a Low Subsonic Wing in Cruise Flight Regime

Muhamad Jayadi*, Rafika Arumsari
Departement of Aeronautical Engineering, Aerospace University of Air Marshal Suryadarma.

Article Info

Article History:
Submitted: December 31, 2024
Revised : January 11, 2025
Accepted : February 28, 2025

Keywords:
Fluid Structure Interaction, Low Sub-Sonic Wing, Lift Coefficient, Drag Coefficient, Safety Factor.

ABSTRACT

This study presents a fluid-structure interaction (FSI) analysis of a low subsonic aircraft wing under cruise conditions. Using computational fluid dynamics (CFD) coupled with structural finite element analysis, the lift and drag coefficients, wing deformation, and structural stresses were simulated over a 5-second interval with a 0.1-second timestep. The simulations revealed that the lift and drag coefficients converged to 0.136 and 0.0456, respectively. Maximum wing deformation was recorded at 4.78 mm, and the highest stress was 2.765 MPa. A calculated safety factor of 309.78 confirms that the wing structure remains well within safe limits under the specified aerodynamic loading. These findings validate the structural integrity of the wing during steady cruise and underscore the effectiveness of FSI simulation in evaluating aeroelastic performance forces

Correspondence Author:
Muhamad Jayadi
Email:
jayadi@unsurya.ac.id

INTRODUCTION

The phenomenon of aeroelasticity has dominated the history of aeronautics since its inception, although aviation pioneers still did not know it thoroughly. Often the desire to conduct further investigation into a phenomenon is triggered by the fear of damage or, in the worst case, catastrophic impact. damage or, in the worst case, catastrophic impact. The failure of the Fokker D.VIII wing box during the First World War may be related to the moment when engineers began to apply the the effects of structural flexibility[1]. Theodorsen's flutter theory in 1935 represented a milestone in the development of numerical tools to study aeroelasticity problems [2]. Experiments helped validate analytical methods that developed in parallel. In 1945 the NACA Langley Research Center built the first wind tunnel for flutter research.

The interaction of fluids with structures is an integral part of the phenomenon of aeroelasticity. Generally, the interaction between fluid and structure often occurs in building structures such as the incident on the Tacoma-Narrow bridge in November 1940[3]. Fluid-structure interaction (FSI) is a multidisciplinary problem that cannot be solved independently. FSI proves that the fluid flow around the structure has a great impact and vice versa. Therefore, changes in the shape of the structure cannot be ignored in terms of fluid flow. The disciplines related to this problem are fluid dynamics and structural dynamics which can be explained through continuum mechanics[3].

The FSI method has been widely used in the last 10 years in a wide variety of applications. Agus et al. (2013) simulated a flapping wing structure by looking at the effect of wing motion on the thrust generated [4]. Junaidin et al. (2014) simulated the wing structure of a high-altitude long endurance (HALE) UAV [5]. This simulation shows the effect of wing deflection on aerodynamic characteristics. Zhang et al. (2018) conducted FSI simulations with Mach number variations from subsonic to hypersonic [6]. Vigneshwaran et al. simulated the AGARD 445.6 wing structure using the one-way FSI method [7].

Nowadays, computational fluid dynamics (CFD) is widely used as a method to analyze aerodynamics characteristics of an object, side by side with analytical and experimental technique. CFD is done by a computer with a software that contains discretized analytical equations and solved by numerical method to find the solution of the governing equations [8].

Wing is the three-dimensional shape of the airfoil that moves through the air so that it interacts with the air and produces lift. Wing design is carried out to produce variations in flying characteristics so that many wings are created with various shapes and sizes [9]. wing is one of the most important part of an airplane. Therefore, this work simulates and analyzes the interactions of an low sub-sonic aircraft's wing structure on aerodynamic forces applied for the aircraft's cruise condition. The wing used for the numerical simulation had a semi span of 13.525m in which the airfoil used was a smoothed low sub-sonic airfoil. The simulation was defined at the cruising flight conditions with a zero angle of attack at an altitude of 18,000 ft and a freestream flow velocity of 141,667 m/s. The simulation was performed with ANSYS Workbench which uses a block transient structure for structural parts and CFX for fluid flow sections which are coupled using a coupling system.

METHODS

2.1 Governing Equation of Fluid Dynamics

The fluid flow's governing equation is in the integral form of the three-dimensional, unsteady, compressible Navier-Stokes equation written in strong conservation form for the moving or deforming control volume given by:

$$\frac{\partial}{\partial t}\int_v WdV + \oint[F - G\}dA = \int_v \boldsymbol{H}dV \qquad (1)$$

where the vectors W (vector of conservative variables), F (vector of convective fluxes) and G (vector of diffusive fluxes) [9] are defined as:

$$W = \begin{Bmatrix} \rho \\ \rho V \\ \rho E \end{Bmatrix} \quad F = \begin{Bmatrix} \rho(V - V_g) \\ \rho(V - V_g) \otimes pI \\ \rho(V - V_g)H + pV_g \end{Bmatrix} \quad G = \begin{Bmatrix} 0 \\ T \\ T.V + q^{"} \end{Bmatrix} \tag{2}$$

and the vector H contains the body forces and energy sources. Here $\boldsymbol{\rho}$, v,V_g,E and pare the density, velocity vector, grid velocity vector, total energy per unit mass and pressure of the fluid respectively. T is the viscous stress tensor and $q^{"}$ is the heat flux. Total energy E and the total enthalpy H is related by E = H – p/ρ where H = h +$|V|^2$ /2 and h = $C_p\ T$. The governing equation is then converted to discrete form by applying it to a cell-centered control volume.

2.2 Governing Equation of Structural Dynamics

The nonlinear differential equations based on the principle of virtual work in combination with finite element method can be written in matrix form as [9]:

$$[M]\{\ddot{u}\} + [C]\{\dot{u}\} + [K]\{u\} = \{F[t]\} \tag{3}$$

where [M], [C] and [K] are the mass, damping and stiffness matrices respectively and {F(t)} is the applied load vector which are due to pressure and shear stress on the wing. {u}, $\{\dot{u}\}$ and $\{\ddot{u}\}$ are the vector of displacement, velocity, and acceleration respectively. Since the geometrically nonlinearities are included in the analysis, the stiffness matrix is a function of the nodal displacements.

2.3 Safety Factor

A structure is declared to have met the safety requirements if the maximum stress that occurs in the structure when operating under normal conditions is still below the yield stress value of the structural material. The level of security of a structure is expressed by a value called the safety factor. Safety actor (SF) is the ratio between the yield stress of the structural material to the maximum stress in the structure when operating normally. The form of the equation of the safety factor is as[10]

$$SF = \frac{\sigma_{ult}}{\sigma_{app}} \tag{4}$$

where σult is Ultimate stress and σapp is the maximum stress, the structure can receive under normal conditions. For the aircraft Have Safety Factor is 1.5-3.5[10]

2.4 Fluid Structure Interaction

Fluid-Structure Interaction (FSI) is the interaction of some movable or deformable structure with an internal or surrounding fluid flow. Fluid-structure interactions can be stable or oscillatory. In oscillatory interactions, the strain induced in the solid structure causes it to move such that the source of strain is reduced, and the structure returns to its former state only for the process to repeat. Fluid-structure interactions are a crucial consideration in the design of many engineering systems, e.g., aircraft, spacecraft, engines, and bridges. Failing to consider the effects of oscillatory interactions can be catastrophic, especially in structures comprising materials susceptible to fatigue[8].

The simulation workflow is starting from fluid modeling and structure modeling shown in **Figure 1**.

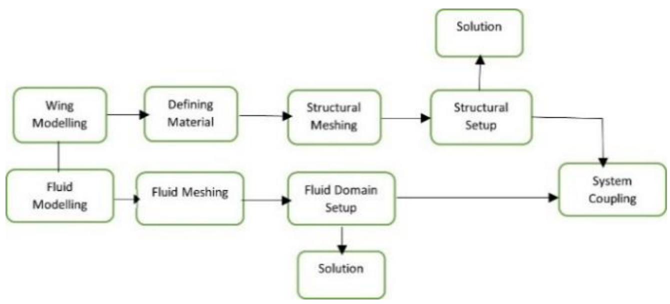

Figure 1. Simulation Workflow FSI

2.5 Structural and Fluid Modeling

The first step of the simulation is to model the fluid domain and the wing geometry. The wing geometry with the airfoil shape and the fluid domain detailed dimensions are as shown in **Figure 2** and **Figure 3** where the wing was defined as a solid.

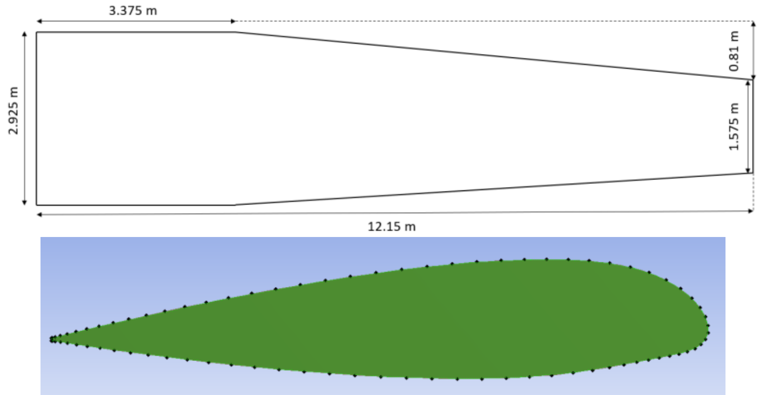

Figure 2. Wing geometry and airfoil shape.

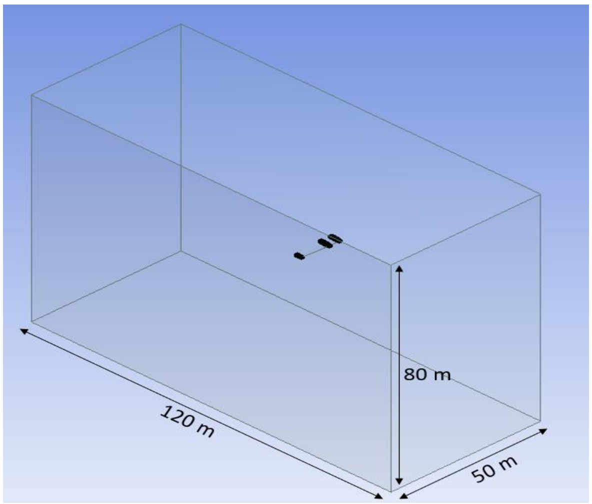

Figure 3. Fluid Domain dimension.

2.6 Material

The wing's material used is Aluminum 2024-T3 which has the material properties as shown in Table 1 below.

Table 1. Aluminum 2024-T3 mechanical properties [11]

Property	**Value**	**Unit**
Density	7850	Kg/m^3
Young Modulus	73.1	GPa
Poisson's Ratio	0.3	-
Ultimate Strength	855	MPa

2.7 Meshing

The wing was then meshed with the size of 0.2 m of patch conforming tetrahedrons. In which the total number of nodes and elements obtained were 792,933 and 284,106 respectively. The average element quality of the structure mesh is 0.624.

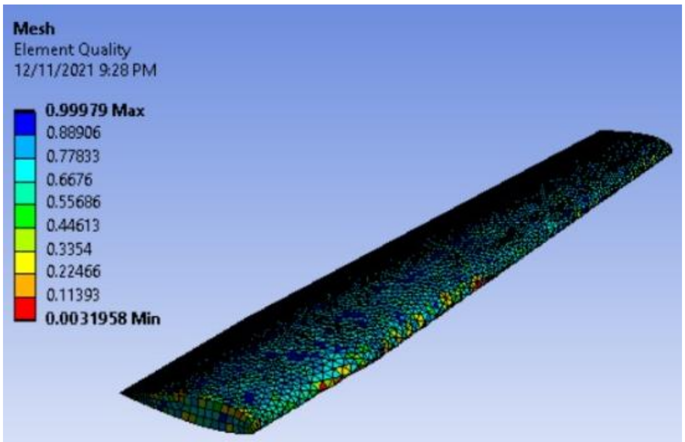

Figure 4. Wing structural mesh

For the fluid domain, the mesh consists of tetrahedrons with size 1 m resulted in 434,890 nodes and 2,406,229 elements with the average element quality of 0.82926. To reduce the computational cost, we decided not to add in an inflation layer as this requires an overall increase the number of elements used with a further decrease in quality.

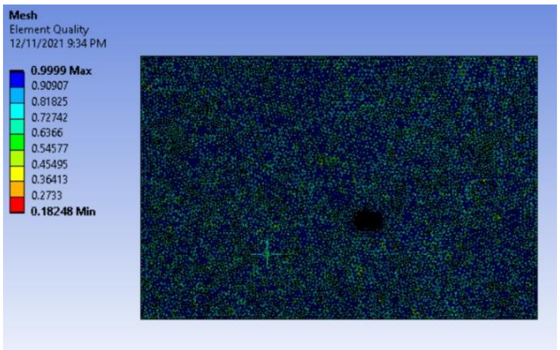

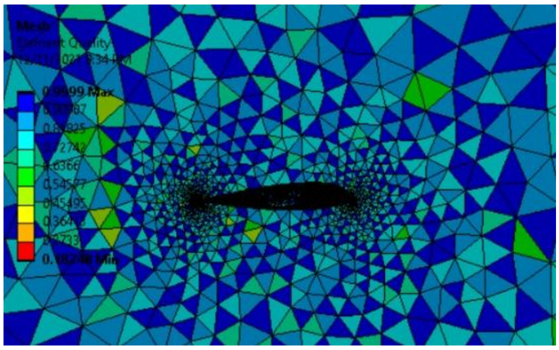

Figure 5. Fluid Domain Mesh

Figure 6. Fluid domain mesh near wing

2.8 Setup

The boundary conditions given for the transient structural analysis was a fixed support boundary condition at the root of the wing and the rest of the wing was set as a fluid-surface interface. The simulation analysis time was calculated up to 5 seconds with a timestep of 0.1 s. Furthermore, as for the fluid domain's material air properties at the cruising condition were used. The boundary conditions at the fluid domain consists of inlet, outlet, symmetry, and farfield as shown in **Figure** 7. For the turbulence model the Shear Stress Transport (SST) model was used. The Air properties at the cruise condition is as given in table 2 below.

Table 2. Air properties at Cruising Condition[12]

Properties	Value	Unit
Altitude	18,000	Ft
Speed	141.774	m/s
Density	0.698145	Kg/m^3
Pressure	50599.8	Pa
Temperature	252.488	K
Specific Heat Capacity	1.003	J/kgK
Dynamic Viscosity	1.62859 x 10-5	Pa s

Thermal Conductivity	0.022475	W/mK

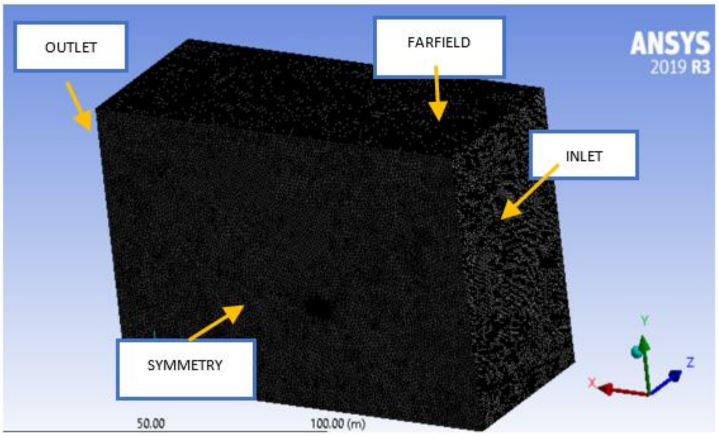

Figure 7. Fluid domain boundary conditions

RESULT AND DISCUSSION

The convergence of the fluid simulation could be observed from the solution's root mean square value reaching 10-8 as shown in **Figure 8**.

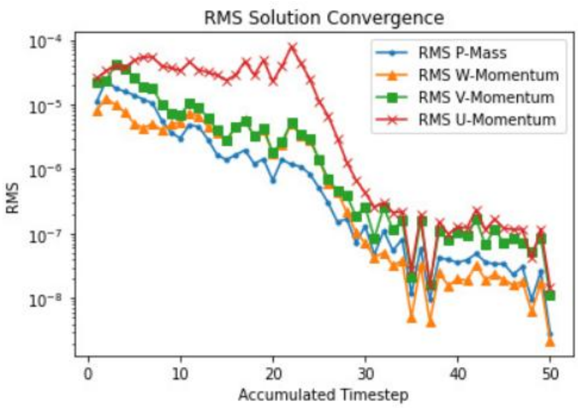

Figure 8. Fluid simulation convergence

From the fluid simulation results of the pressure and velocity contour plot shown in **Figure 9** and **Figure 10**, it could be observed that a larger velocity occurs at the upper surface of the airfoil thus creating a lower pressure at the upper surface that induced lift force on the wing. Where there is a minimum relative pressure of -6.173kPa creating suction at the upper surface of the airfoil and the largest pressure of 8.893 kPa at the airfoil's leading edge stagnation point. Also, the maximum velocity at the upper surface of the wing reaches 176.4 m/s.

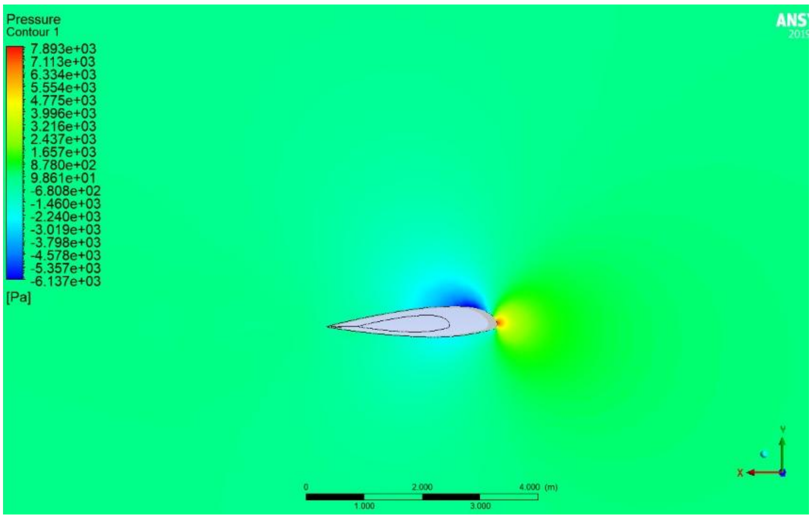

Figure 9. Pressure distribution at XY plane

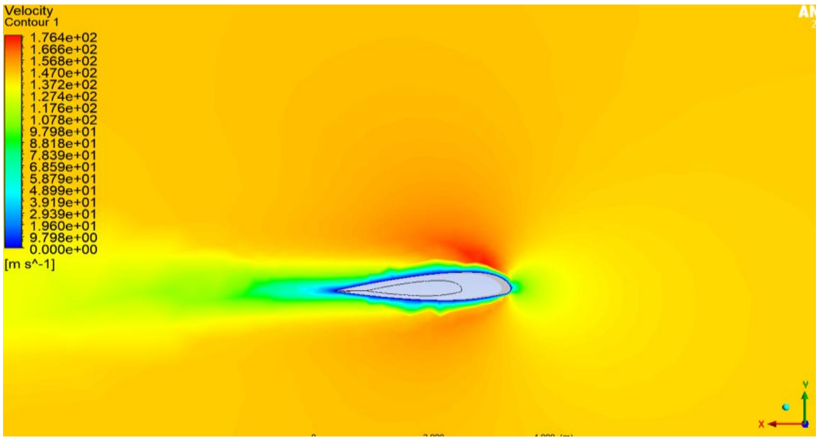

Figure 10. Velocity distribution at XY plane

As for the wing structure simulation, the results show that the maximum deformation happens at the tip of the wing that achieved a displacement of 4.783 mm as shown in **Figure 11**. Also, there would be no deformation at the root of the wing as it is a fixed support not moving against the fuselage of the aircraft.

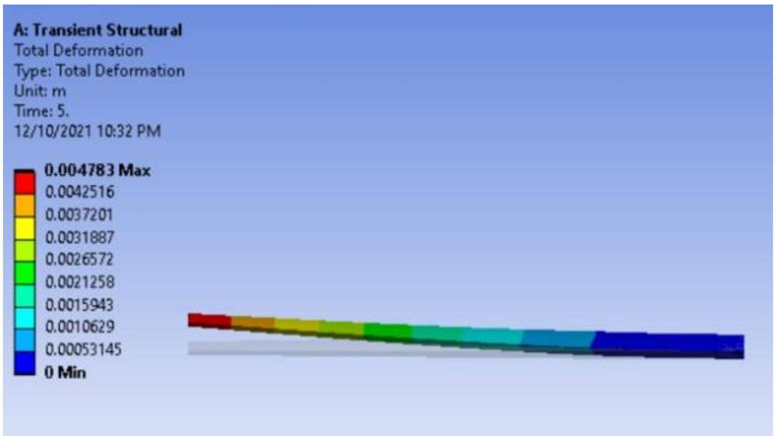

Figure 11. Wing structural displacement distribution

As for the stress distribution of the wing, **Figure 12** shows the resulting von mises stress distribution and it shows that the maximum stress occurs at the root of the wing at a value of 2.765 MPa. This happens due to the fixed support role of the root of the wing. Then, to validate that the wing structure is in a safe condition, the safety factor of the wing was calculated and the value of the safety factor obtained is 309.78. This value indicates that the structure is safe condition. This value of safety factor is considered quite too large as commonly it is around 1.5. But this happens as it is assumed that the simulated condition in this work is only on a normal loading at cruise condition where the loading could be quite different if the aircraft performs maneuvers resulting in a much larger wing loading.

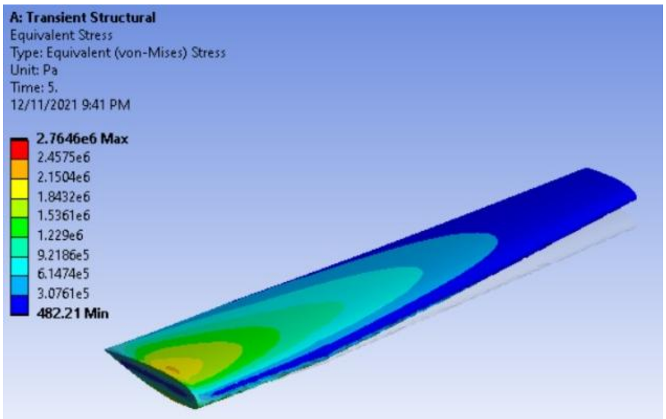

Figure 12. Von mises stress distribution

The results of the drag and lift coefficient along the simulated 5s are as shown in **Figure 13** and **Figure 14**. The results show that the wing starts to become stable at 1.5s of the simulation where the drag and lift coefficients starts to converge. This also could be observed from the plot of the maximum structural stress shown in **Figure 15**.

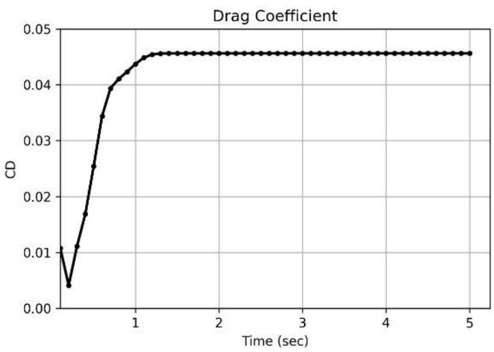

Figure 13. Drag Coefficient from t= 0s

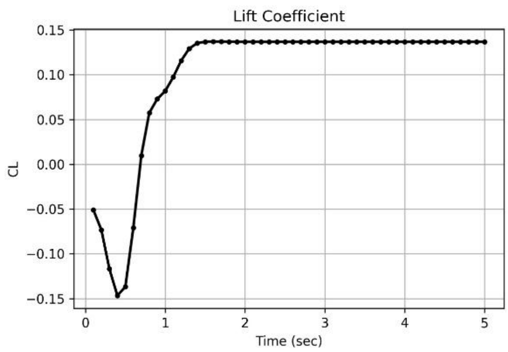

Figure 14. Lift Coefficient from t= 0s

Although the previous plots showed that the solution converges to a single value, if the drag and lift coefficient and also the maximum stress are plotted with a magnified scale of the y axis, an oscillatory motion could be observed happening at the wing that slowly converges to a value. The plot of magnified scale could be seen as shown in **Figure 16, Figure 17 and Figure 18** respectively.

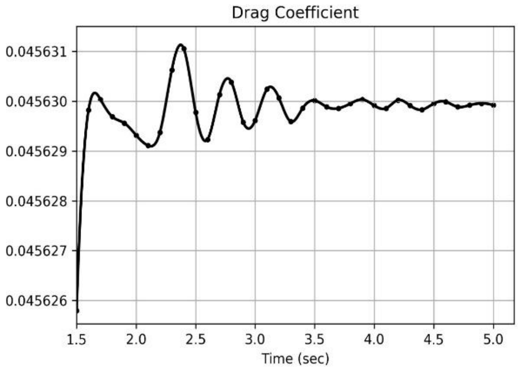

Figure 16. Drag coefficient from t= 1.5s

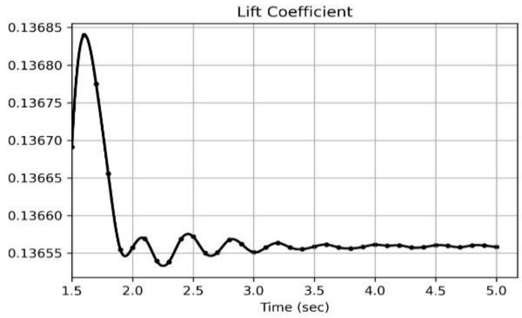

Figure 17. Lift coefficient from t= 1.5s

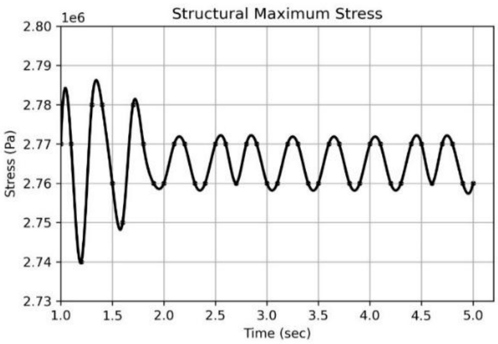

Figure 18. Maximum stress from t= 1s

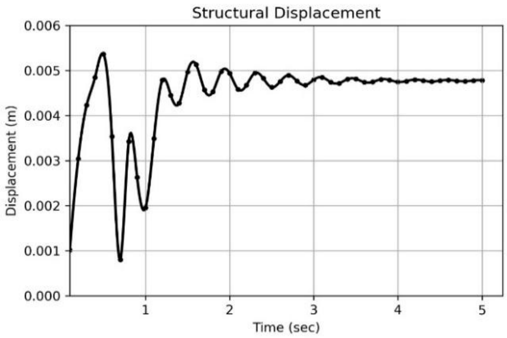

Figure 19. Structural displacement from t=0s

The results show that the drag coefficient converges to 0.04563, lift coefficient to 0.13656, structural maximum stress to 2.765 MPa, and a maximum structural displacement of 4.783 mm.

.

CONCLUSION

This study successfully employed fluid-structure interaction simulation to analyze the structural response of low subsonic aircraft wing under cruise flight conditions. The simulation demonstrated stable aerodynamic performance, with lift and drag coefficients converging to 0.13656 and 0.04563, respectively. Structural analysis showed a maximum displacement of 4.783 mm at the wing tip and a peak von Mises stress of 2.765 MPa at the root. The resulting safety factor of 309.78 suggests that the wing design is highly conservative for the given cruise condition. This unusually high value may indicate that the simulated loading conditions are significantly lower than the actual operational loads or that the model simplifies certain dynamic effects, potentially overestimating structural robustness. for the given cruise condition. While the structure remains safe, the exceptionally high safety factor highlights the need for further investigation under varied flight conditions, including maneuvers and turbulent loads. Future work should focus on expanding the flight envelope, refining boundary conditions, and validating simulation results with experimental or empirical data. The current study lacks validation against physical tests or flight data, which is essential to ensure the reliability and applicability of the simulation outcomes. with experimental or empirical data to enhance model credibility and practical relevance.

BIBLIOGRAPHY

[1] U. Cella, Setup and Validation of High-Fidelity Aeroelastic Analysis Methods Based on RBF Mesh Morphing, M.S. thesis, Universita Degli Studi Di Roma “Tor Vergata,” 2015.

[2] T. Theodorsen, “General theory of aerodynamic instability and the mechanism of flutter,” NACA Report, no. 496, 1936.

[3] F. Benra, H. J. Dohmen, J. Pei, S. Schuster, and B. Wan, “A comparison of one-way and two-way coupling methods for numerical analysis of fluid structure interactions,” Journal of Applied Mathematics, vol. 2011, pp. 1–16, 2011, doi: 10.1155/2011/853560.

[4] D. A. Priyanto, “Simulasi interaksi fluida dan struktur sayap kepak,” Undergraduate thesis, Dept. Teknik Dirgantara, Institut Teknologi Bandung, Indonesia, 2013.

[5] B. Junaidin, “Numerical simulation of flexible wing of HALE UAV using two-way fluid structure interaction method,” Undergraduate thesis, Dept. Teknik Dirgantara, Institut Teknologi Bandung, Indonesia, 2014.

[6] L. Zhang and C. Sun, “Simulation analysis of fluid-structure interaction of high velocity environment influence on aircraft wing materials under different Mach numbers,” Sensors, vol. 18, no. 4, p. 1248, 2018, doi: 10.3390/s18041248.

[7] V. Vigneshwaran, S. Vijayaraghavan, G. Sivamanikandan, M. K., K. Keerthana, and K. Balaji, “Fluid-structure interaction over an aircraft wing,” International Journal of Engineering Research and Development, vol. 13, no. 4, pp. 27–31, Apr. 2017. [Online]. Available: www.ijerd.com

[8] M. Ezkurra et al., “Analysis of one-way and two-way FSI approaches to characterize the flow regime and the mechanical behaviour during closing manoeuvring operation of a butterfly valve,” International Journal of Mechanical and Materials Engineering, vol. 13, no. 1, pp. 1–15, 2018.

[9] A. A. Kumar et al., “Fluid-structure interaction analysis of a cropped delta wing,” in Proc. 12th Int. Conf. on Vibration Problems (ICOVP), 2016.

[10] J. W. Bristow et al., “Safety factors in civil aircraft design requirements,” Engineering Failure Analysis, vol. 14, no. 3, pp. 459–470, 2007.

[11] ASM Material Data Sheet, “Aluminum 2024-T3,” MatWeb, [Online]. Available: http://asm.matweb.com/search/SpecificMaterial.asp?bassnum=ma2024t3 [Accessed: Nov. 28, 2021].

[12] M. F. Nita, Aircraft Design Studies Based on the ATR 72, Hamburg University of Applied Sciences, 2008.